ORIGINAL PAPER

Nagoya J. Med. Sci. **87**. 787–800, 2025
doi:10.18999/nagjms.87.4.787

Human dental pulp stem cells-derived small extracellular vesicles prevent osteoradionecrosis of the jaw in a rat model

Go Ohara[1,2], Kazuto Okabe[1,3], Kotaro Sato[1], Naoto Toyama[1,4], Yuya Ohta[1,5], Kento Kaminogo[6], Junna Watanabe[6], Norihisa Ichimura[1,2], Kiyoshi Sakai[6] and Hideharu Hibi[1,6]

[1]*Department of Oral and Maxillofacial Surgery, Nagoya University Graduate School of Medicine, Nagoya, Japan*
[2]*Department of Oral and Maxillofacial Surgery, Komaki City Hospital, Komaki, Japan*
[3]*Department of Oral and Maxillofacial Surgery, Nagoya City University Graduate School of Medical Science, Nagoya, Japan*
[4]*Department of Oral and Maxillofacial Surgery, Iwata City Hospital, Iwata, Japan*
[5]*Department of Oral and Maxillofacial Surgery, Chutoen General Medical Center, Kakegawa, Japan*
[6]*Department of Oral and Maxillofacial Surgery, Nagoya University Hospital, Nagoya, Japan*

ABSTRACT

Radiotherapy (RT) is an important standard treatment for head and neck cancer. On the other hand, osteoradionecrosis of the jaw (ORNJ), a side effect of RT, is intractable and has been a long-standing problem that needs to be overcome. Cellular senescence has been linked to the development of ORNJ; however, strategies for preventing and treating this disease have not been established. This study aimed to evaluate the effects of human dental pulp stem cell-derived small extracellular vesicles (hDPSC-sEV) on ORNJ. The effects of hDPSC-sEV treatment on rat bone marrow cells (rBMC) were examined in vitro. In addition, hDPSC-sEV were administered intravenously to a rat ORNJ model, and the extraction socket was examined radiologically and histologically. In vitro, rBMC treated with hDPSC-sEV immediately after irradiation showed downregulated expression of senescence-related genes. In vivo, the extraction sockets of the ORNJ models treated with hDPSC-sEV showed more new bone and greater coverage with gingiva relative to those observed in the comparison groups. This study suggests that hDPSC-sEV may inhibit ORNJ development. One possible mechanism is that hDPSC-sEV inhibit radiation-induced cellular senescence.

Keywords: cellular senescence, dental pulp stem cells, extracellular vesicle, osteoradionecrosis of the jaw, radiotherapy

Abbreviations:
BMC: bone marrow cells
BMSC: bone marrow stem cells
CNT: control
DPSC: dental pulp stem cells
MSC: mesenchymal stem cells
ORNJ: osteoradionecrosis of the jaw
RT: radiotherapy
sEV: small extracellular vesicles
PBS: phosphate-buffered saline
mRNA: messenger RNA

Received: December 26, 2024; Accepted: May 16, 2025
Corresponding Author: Go Ohara, DDS, PhD
Department of Oral and Maxillofacial Surgery, Nagoya University Graduate School of Medicine,
65 Tsurumai-cho, Showa-ku, Nagoya 466-8550, Japan
Tel: +81-52-744-2348, Fax: +81-52-744-2352, E-mail: g.ohara@komakihp.gr.jp

INTRODUCTION

Radiotherapy (RT) is one of the effective treatments for head and neck cancer, along with surgery and chemotherapy, helping preserve the maxillofacial function and esthetics.[1] However, RT can cause adverse effects in the oral cavity, whose healthy tissues are included in the irradiation field. Bone tissue is susceptible to damage that can present as osteoradionecrosis of the jaw (ORNJ), which is difficult to treat. Osteoradionecrosis can be defined as ischemic osteonecrosis caused by irradiation, and its diagnosis is based on clinical findings such as signs of necrosis and exposure of irradiated bone, prolonged or disrupted healing, and local tumor necrosis and recurrence, without any evidence of metastasis.[2] Despite the use of novel techniques, such as intensity-modulated proton therapy, designed to reduce risks to healthy tissues, the estimated incidence of ORNJ remains at 78%.[3,4] ORNJ can lead to maxillofacial tissue damage and pathological fractures. It can also cause poor oral intake and malnutrition, significantly reducing patient quality of life.[2] It is a long-term condition that is currently considered irreversible.

Treatment for ORNJ is determined by disease stage and classification,[5] as well as patient characteristics, including age, compliance, and access to interventions. Based on the degree of bone and soft tissue damage, ORNJ can be classified into four stages (stages 0–III).[6] Early-stage disease can be treated with chlorhexidine washing, antibiotics, and analgesics.[5] Late-stage ORNJ requires additional surgical treatment, such as sequestrum removal, marginal mandibulectomy, segmental mandibulectomy, radical resection, and flap reconstruction, alongside conservative treatments.[5] These treatments are more symptomatic than radical treatments for this disease. Risk factors associated with the development of ORNJ have not yet been defined, however, one of the most important risk factors is the patient extractions after RT.[7] Many clinicians tend to leave a tooth rather than extract it, even for a tooth with a poor prognosis, in order to avoid developing ORNJ by their own procedures. However, this is not a fundamental solution, because the risk of developing ORNJ remains due to leaving the tooth as a source of infection. Therefore, preventive and treatment strategies for ORNJ are required.

Mesenchymal stem cells (MSC) have been used in regenerative medicine studies. MSC secrete various cytokines to regulate immune cell and growth factor expression, promoting the regeneration of damaged tissue, including in radiation-induced bone injury.[8,9] Using swine and rat ORNJ models, several studies have shown the feasibility and clinical efficacy of MSC, including those derived from human umbilical cord blood and tonsils, in the treatment of radiation-induced bone damage.[10-12] These effects of MSC may be mediated by small extracellular vesicles (sEV) released by the stem cells, which exert paracrine effects and are defined as less than 200 nm in diameter.[13] sEV contribute to intercellular communication by transferring cytosolic proteins, lipids, and RNA from cell to cell.[14,15] sEV-based therapies have various advantages over stem cell-based therapies, such as non-self-replicating secretions, lack of multiple lineage differentiation abilities, rapid preparation, and reduced expansion during preservation and preparation, and have been evaluated for the diagnosis and treatment of various diseases. Bone marrow stem cells-derived sEV (BMSC-sEV) promote bone regeneration in a rat model of osteonecrosis of the femoral head.[16] Furthermore, the bone-healing effect of BMSC-sEV in the jawbone after tooth extraction may help prevent the development of bisphosphonate-associated osteonecrosis of the jaw.[17] These reports suggest that BMSC-sEV may have an effect on suppressing cellular senescence. However, no reports confirm this effect in the ORNJ model.

Extracted teeth are a valuable source of stem cells and have been used in tissue-derived stem cell therapy research.[18] Among them, dental pulp stem cells (DPSC) are less invasive to extract than other stem cell types, and raise fewer ethical concerns because they are isolated from teeth removed during routine dental procedures.[19] Most importantly, DPSC have therapeutic efficacy

comparable to or better than that of BMSC.[19] Previous studies have shown their efficacy in suppressing inflammation, protecting against neurodegeneration, and treating periodontitis.[20-22] In addition, DPSC-sEV may restore salivary gland dysfunction caused by radiation injury.[23] However, the effects of DPSC-sEV on ORNJ remain unknown. In this study, we injected human DPSC-sEV (hDPSC-sEV) into a rat model of ORNJ and aimed to evaluate their effects on wound healing and target cells using histological, radiological, and molecular biology analyses.

MATERIALS AND METHODS

Isolation and characterization of hDPSC-sEV

hDPSC were purchased from Lonza (PT-5025; Basel, Switzerland) and cultured in Dulbecco's modified Eagle medium (Sigma-Aldrich, St. Louis, USA) containing 10% fetal bovine serum (GE Healthcare Bioscience, Little Chalfont, UK) and 1% penicillin-streptomycin (Fujifilm-Wako, Osaka, Japan) at 37 °C in a 5% CO_2 incubator. hDPSC-sEV were isolated, following previously reported methods.[17,23] The isolated hDPSC-sEV were visualized under a transmission electron microscope (TEM; JEM-1400PLUS, JEOL, Tokyo, Japan). Nanoparticle tracking analysis (NTA) was performed using a Nanosight system (Malvern Instruments, Amesbury, UK), and the recorded 60 s videos were analyzed using NTA software (version 3.4).

Irradiation of rat bone marrow cells

Rat bone marrow cells (rBMC) were collected from the femurs of four-week-old male Sprague–Dawley rats[24] and used for up to three passages. rBMC were cultured in Dulbecco's modified Eagle medium supplemented with 10% fetal bovine serum and 1% penicillin-streptomycin and divided into three groups: control (CNT) group, no irradiation and co-cultured with phosphate-buffered saline (PBS); RT group, irradiated with 6 Gy and co-cultured with PBS; and RT+sEV group, irradiated with 6 Gy and co-cultured with hDPSC-sEV. Cells were irradiated with a single 6 Gy dose at a rate of 0.57 Gy/min using an X-ray irradiation system (MBR-1520R-3; Hitachi Power Solutions, Tokyo, Japan), and then the RT+sEV group was immediately co-cultured with hDPSC-sEV (10 μg/mL) suspended in 500 μL PBS. After 48 h of co-culture, the medium of each group was replaced. The cells were then cultured for a predetermined period and either collected or used for subsequent experiments.

Senescence-associated β-galactosidase staining

Senescence-associated β-galactosidase (SA-β-gal) staining kit (SPiDER-βGal; DOJINDO) was used according to the manufacturer's protocol. The cells were seeded in 12-well plates at a density of 5×10^3 cells/well, cultured for 24 h, and irradiated. After 24 h of incubation, the cells were fixed in 4% paraformaldehyde (PFA). The cells were then stained with X-gal solution for 24 h, and observed and compared for relative brightness standardized by 4′,6-diamidino-2-phenylindole, using a BZ-X800 all-in-one fluorescence microscope and analyzer (Keyence, Osaka, Japan).

Cell proliferation assay

Cell proliferation assays followed previously reported methods.[25] Briefly, a Cell Counting Kit-8 (Dojindo Laboratories, Kumamoto, Japan) was used according to the manufacturer's instructions.

Colony formation assay

Cells were seeded in 6-well plates at a density of 1×10^4 cells/well and pre-cultured for 24

h. After treatment, the cells were cultured for another 14 days and fixed in 4% PFA. The cells were stained with 2% crystal violet, a 70% methanol solution was added, and the cells were allowed to stand. Stained cells were observed using BZ-X800. In addition, the extracted crystal violet was stirred to ensure uniformity, and the absorbance was measured at 590 nm using an Infinite 200 PRO system and i-control software (Tecan Japan Co, Ltd, Kanagawa, Japan).

Real-time reverse transcriptase-polymerase chain reaction

Quantitative real-time reverse transcriptase-polymerase chain reaction (RT-PCR) analyses were performed as previously described.[26] Briefly, TRIzol LS Reagent (Thermo Fisher Scientific), ReverTra Ace qPCR RT Master Mix, gDNA Remover (Toyobo Co, Ltd, Osaka, Japan), THUNDERBIRD SYBR qPCR Mix (Toyobo), and AriaMx RT-PCR System (Agilent Technologies International Japan, Ltd, Tokyo, Japan) were used according to the manufacturer's instructions. Primer sequences are listed in the Table.

Table PCR primer sequences

Primer	Sequence (forward 5′-3′)	Sequence (reverse 5′-3′)
p16	GTCACACGACTGGGCGATTG	AGTCTGTCTGCAGCGGACTC
p21	AGTAGACACGAAACAGGCTCAG	TCAACACCCTGTCTTGTCTTCG
RUNX2	CACTGACTCGGTTGGTCTCG	CACAAGTGCGGTGCAAACTT
OPN	ACAGTATATCCCGATGCCACAG	GACCACGAGGTTGGGATGAC
OCN	TCAGACGGAAGCTGCAGAA	TTTTCAGCCACCACCTCCTC
BMP2	TTAAGACGCTTCCGCTGTTT	GTTTGGCCTGAAGCAGAGAC
PPARG	ATTGAGTGCCGAGTCTGTGG	GCTTCAATCGGATGGTTCTTCG
Ebf1	ACAAGTCCAAGCAGTTCTGC	TGTAACCTCTGGAAGCCGTAG
GAPDH	AACTTTGGCATCGTGGAAGG	CGGATACATTGGGGGTAGGA

p16: cyclin-dependent kinase inhibitor 2A
p21: cyclin-dependent kinase inhibitor 1A
RUNX2: runt-related transcription factor 2
OPN: osteopontin
OCN: osteocalcin
BMP2: bone morphogenetic protein-2
PPARG: peroxisome proliferator-activated receptor gamma
Ebf1: early B-cell factor 1
GAPDH: glyceraldehyde-3-phosphate dehydrogenase
PCR: polymerase chain reaction

Animals

All animal studies were approved by Nagoya University School of Medicine Animal Care and Use Committee (nos. 31081, 20245, 210698, and 220186) and were conducted in accordance with Guidelines for Animal Experiments of Nagoya University Graduate School of Medicine. The rat ORNJ model was established as previously described.[27,28] Seven-week-old male Sprague–Dawley rats (Japan SLC, Inc) were randomized into three groups (n = 3): CNT group, rats with no irradiation and injected with PBS; RT group, rats that received 20 Gy irradiation and injected

with PBS; and RT+ sEV group, rats that received 20 Gy irradiation and injections with hDPSC-sEV. The left mandible of the rat was irradiated with a single 20 Gy dose at a rate of 0.57 Gy/min using an X-ray irradiation system on day 0; the rest of the rat's body was shielded by a lead block. After irradiation, the RT+sEV group immediately injected an hDPSC-sEV (1.6 mg/kg) through the tail vein (suspended in 500 μL PBS). On day 10, three molars on the left side were extracted from all groups. On day 31, the rats were anesthetized and euthanized, and their mandibular bones were harvested for histological and radiological analyses. All experiments were n = 3 per group.

Histology

The rat mandible was fixed in 4% PFA for 24 h, decalcified for 6 weeks with 10% ethylenediaminetetraacetic acid, and sliced into 4-μm thick sections. Sections were stained with hematoxylin and eosin (Muto Pure Chemicals, Tokyo, Japan). Tissue images were captured using a fluorescence microscope (BZ-800; Keyence, Osaka, Japan).

Microtomography and bone mineral density analysis

The rat mandible was imaged using Latheta LCT-200 (Hitachi Aloka Medical, Tokyo, Japan), a three-dimensional reconstructed microtomography (μCT) designed for laboratory animals. A detailed analysis of the bone quality was conducted on the second molar, using a range of 60 slices of 48-μm thickness, with the aid of VGSTUDIO 3.4 (VOLUME GRAPHICS, Aichi, Japan).

Statistical analysis

All statistical analyses were performed using Prism (version 10; GraphPad Software, San Diego, CA, United States). Welch's t-test was used to determine *P*-values. One-way analysis of variance was used for multiple comparisons, followed by Tukey's test. Results are expressed as the mean ± standard deviation of at least three independent experiments. The results were considered statistically significant at $P < 0.05$.

RESULTS

Isolation and identification of hDPSC-sEV

The isolated hDPSC-sEV fraction was assessed using NTA and TEM to ensure that high-quality samples were obtained. NTA showed that the vesicle sizes were distributed between 50 and 200 nm in diameter. The most common diameter value was 98 nm (Figure 1A). The TEM images confirmed the presence of circular membranous vesicles (Figure 1B). These results were consistent with those of our previous study, in which hDPSC-sEV were collected using a similar method.[23] Therefore, we decided to use this sample in this study.

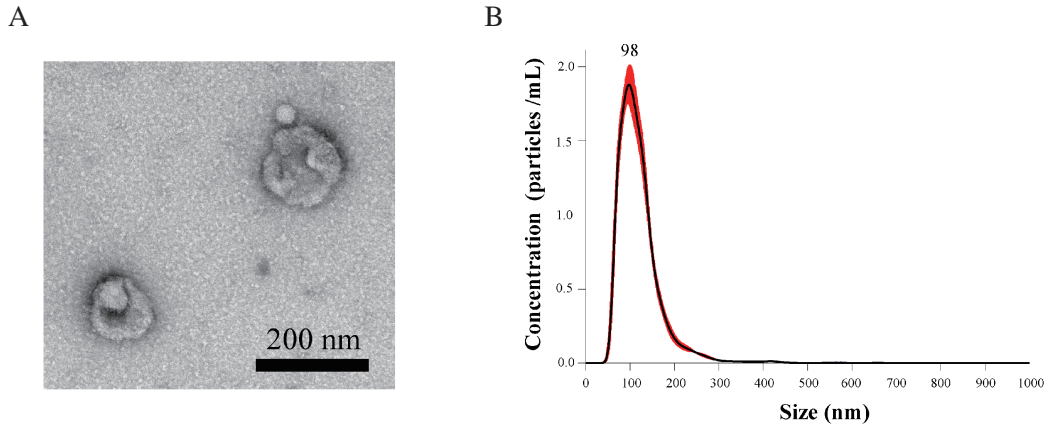

Fig. 1 Identification of human dental pulp stem cell-derived small extracellular vesicles
Fig. 1A: Representative image of purified human dental pulp stem cells-derived small extracellular vesicles (hDPSC-sEV) obtained using transmission electron microscopy; scale bar, 200 nm.
Fig. 1B: Particle size distribution of hDPSC-sEV measured using a Nanosight system.

hDPSC-sEV suppress radiation-induced cellular senescence of BMC in vitro

Initially, we evaluated the effects of hDPSC-sEV in vitro. The expression of β-galactosidase, which is unique to senescent cells, was enhanced by approximately 2.5-fold in the RT group compared with that in the CNT group. In contrast, the expression of β-galactosidase was significantly attenuated in the RT + sEV group compared to that in the RT group, although both groups showed enhanced values compared with those in the CNT group (Figure 2A). In the cell proliferation assay using WST-8, the RT group showed a significant 0.7-fold decrease in cell proliferation compared with the CNT group. However, the RT+sEV group showed a greater extent of proliferation than that observed in the RT group, which was also 0.8-fold greater than that in the CNT group (Figure 2B). In the colony formation assay, the RT group showed a 0.1-fold decrease in colony formation compared with the CNT group. In contrast, the RT+sEV group proliferated significantly more than the RT group and approximately 0.3-fold more than the CNT group (Figure 2C). Furthermore, the messenger RNA (mRNA) expression related to cellular senescence increased approximately 4-fold for *cyclin-dependent kinase inhibitor 2A (p16)* and 2-fold for *cyclin-dependent kinase inhibitor 1A (p21)* in the RT + PBS group compared to those in the CNT group and the mRNA expression in the RT + sEV group was comparable to the CNT group (Figure 2D). Following the evaluation of cellular senescence, we evaluated the expression of genes related to bone and fat differentiation in rBMC. The expression levels of mRNAs related to osteogenic differentiation, such as *runt-related transcription factor 2 (RUNX2)*, *osteopontin (OPN)*, *osteocalcin (OCN)*, and *bone morphogenetic protein-2 (BMP2),* were upregulated approximately 1.5–2.5-fold in the RT+sEV group compared to those in the RT group. Meanwhile, the expression of mRNAs related to adipogenic differentiation, such as *peroxisome proliferator-activated receptor gamma (PPARG)* and *early B-cell factor 1* (*Ebf1*), was upregulated approximately 2.5-fold in the RT group compared with those in the CNT and RT + sEV groups (Figure 2E).

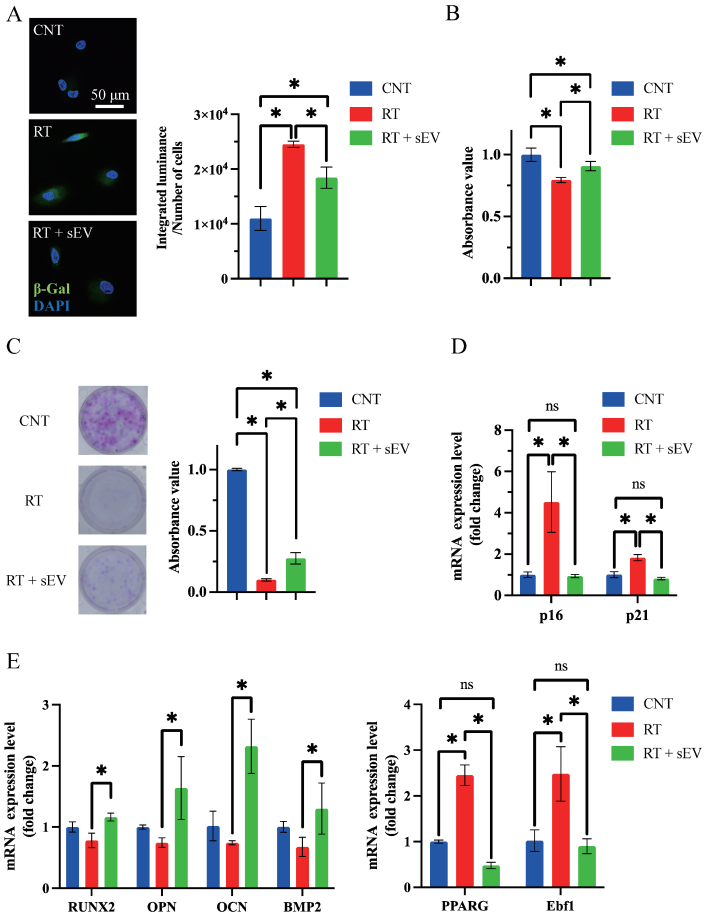

Fig. 2 Effects of human dental pulp stem cell-derived small extracellular vesicles on irradiated bone marrow cells in vitro

Fig. 2A: Evaluation of cellular senescence by senescence-associated β-galactosidase (SA-β-gal) staining (green); scale bar: 50 μm. Blue indicates 4′,6-diamidino-2-phenylindole. Graph presents quantified relative intensities of staining.

Fig. 2B: Cell proliferation assay as determined using the Cell Counting Kit-9.

Fig. 2C: Colony formation, as assessed by crystal violet staining. Graph of quantified relative staining intensities.

Fig. 2D: Relative intensity of messenger RNA (mRNA) expression associated with cellular senescence as determined using reverse transcriptase-polymerase chain reaction (RT-PCR).

Fig. 2E: Relative intensity of mRNA expression associated with osteogenic and adipogenic differentiation as determined using RT-PCR.

All experiments were performed in rat bone marrow cells collected from the femurs. Control (CNT) group, no irradiation and co-cultured with phosphate-buffered saline (PBS); Radiotherapy (RT) group, irradiated with 6 Gy and co-cultured with PBS; RT+sEV group, irradiated with 6 Gy and co-cultured with human dental pulp stem cells-derived small extracellular vesicles (hDPSC-sEV). n = 3/group. Error bars indicate the SEM. *$P < 0.05$.

DAPI: 4′,6-diamidino-2-phenylindole

RUNX2: runt-related transcription factor 2

OPN: osteopontin

OCN: osteocalcin

BMP2: bone morphogenetic protein-2

PPARG: peroxisome proliferator-activated receptor gamma

Ebf1: early B-cell factor 1

ns: not significant

hDPSC-sEV promote wound healing of extraction sockets in the rat ORNJ model

To further evaluate the effects of hDPSC-sEV, in vivo experiments were performed using a rat bisphosphonate-related osteonecrosis of the jaw (BRONJ) model. The rats were irradiated, and their teeth were extracted according to the schedule (Figure 3A). The body weights of the rats in the three groups were monitored continuously throughout the study period. Although the RT and RT+sEV groups developed mandibular alopecia and oral mucositis a few days after RT, no significant weight loss due to decreased food intake was observed (Figure 3B). Three weeks after tooth extraction, the mandibles were removed and histologically analyzed. The CNT group had 92.5% of the extraction socket covered by periodontal tissue, whereas the RT group had only 58.1% coverage and discernible exposure of the alveolar bone (Figure 3C, D). In contrast, in the RT+sEV group, 78.2% of the extraction socket was covered by periodontal tissue, with only some exposure to the alveolar bone (Figure 3C, D). Furthermore, hematoxylin and eosin staining of the mandibular second molar sections showed a loss of epithelial continuity in the extraction socket in the RT group (Figure 3E). Additionally, serrated bone resorption was observed and the bone marrow was fibrotic (Figure 3E, F). In contrast, the RT+sEV group showed epithelial continuity and the same bone trabecular tissue development as the CNT group (Figure 3E, F). In the RT group, adipose marrow in the extraction socket, inflammatory cell infiltration, and a few new capillaries were observed (Figure 3E, F).

hDPSC-sEV promote bone tissue formation in extraction sockets in the rat ORNJ model

Furthermore, bone quality of the mandible was evaluated radiographically in each group. Three weeks after tooth extraction, the corresponding extraction sockets were compared among the three groups using μCT. The RT group had less bone tissue formation than the CNT group. However, the RT + sEV group showed increased and decreased bone tissue build-up compared to those in the RT and CNT groups, respectively (Figure 4A). Trabecular bone mineral density and bone volume/tissue volume were significantly decreased in the RT group compared to those in the CNT group, whereas they did not differ in the RT + sEV group (Figure 4B). The cortical bone mineral density did not show a clear difference among the three groups (Figure 4B).

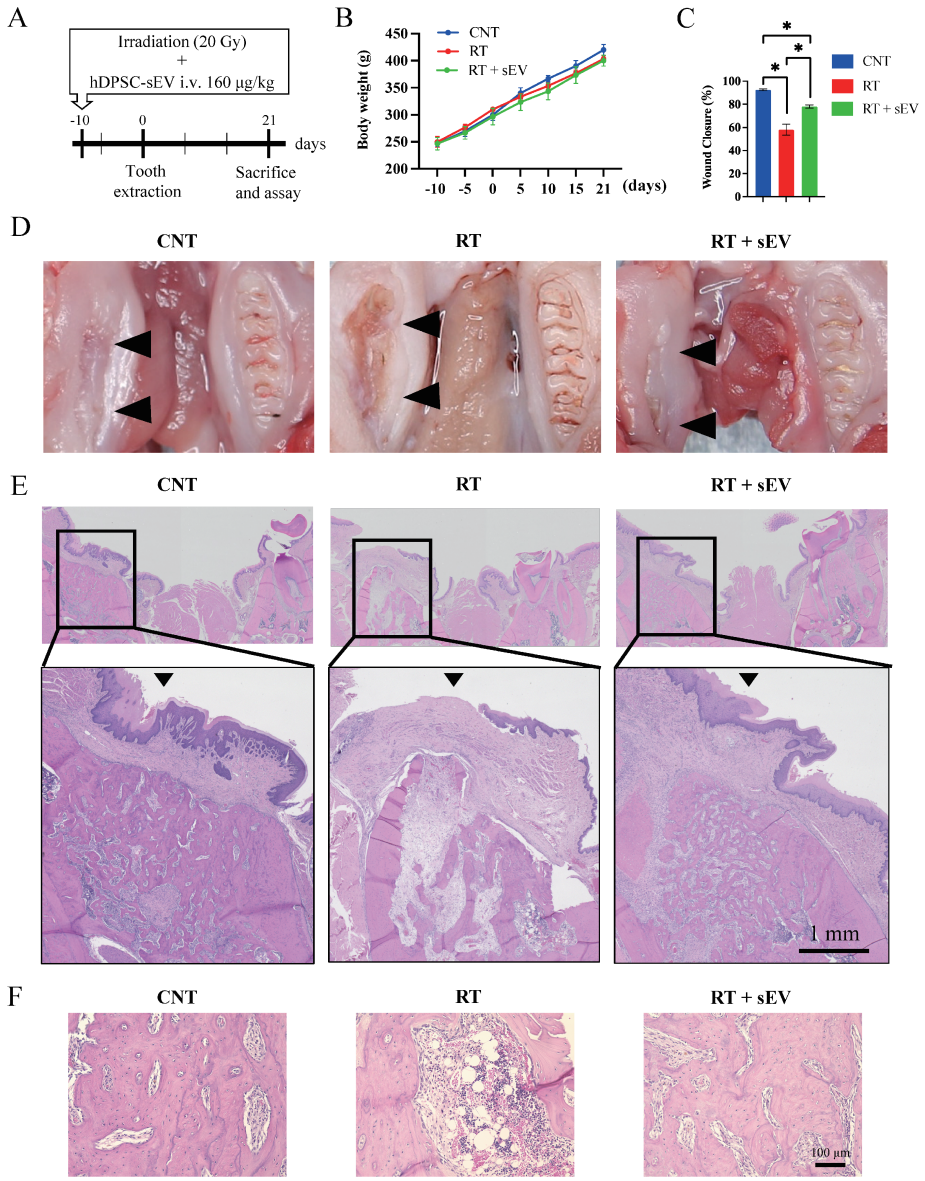

Fig. 3 Histological evaluation of extraction socket in rat osteonecrosis of the jaw model

Fig. 3A: Schedule for developing rat osteonecrosis of the jaw (ORNJ) model and injecting human dental pulp stem cells-derived small extracellular vesicles (hDPSC-sEV).

Fig. 3B: Mean values of body weight variation were obtained every 5 days for each group.

Fig. 3C: Graph showing the degree of wound closure.

Fig. 3D: Images of a representative mandible specimen. Black arrowheads indicate the tooth-extracted parts.

Fig. 3E: Representative hematoxylin and eosin staining images of the mandible. Black arrowheads indicate enlarged images of the tooth-extracted parts. Scale bar, 1 mm.

Fig. 3F: Representative high-magnification tissue image of the mandible. Scale bar: 100 μm.

All mandibles were evaluated 3 weeks after extraction. Control (CNT) group, rats with no irradiation and injected phosphate-buffered saline (PBS); Radiotherapy (RT) group, rats received 20 Gy irradiation and injected PBS; RT+ sEV group, rats received 20 Gy irradiation and injected hDPSC-sEV. n = 3/group. Error bars indicate the SEM. $*P < 0.05$.

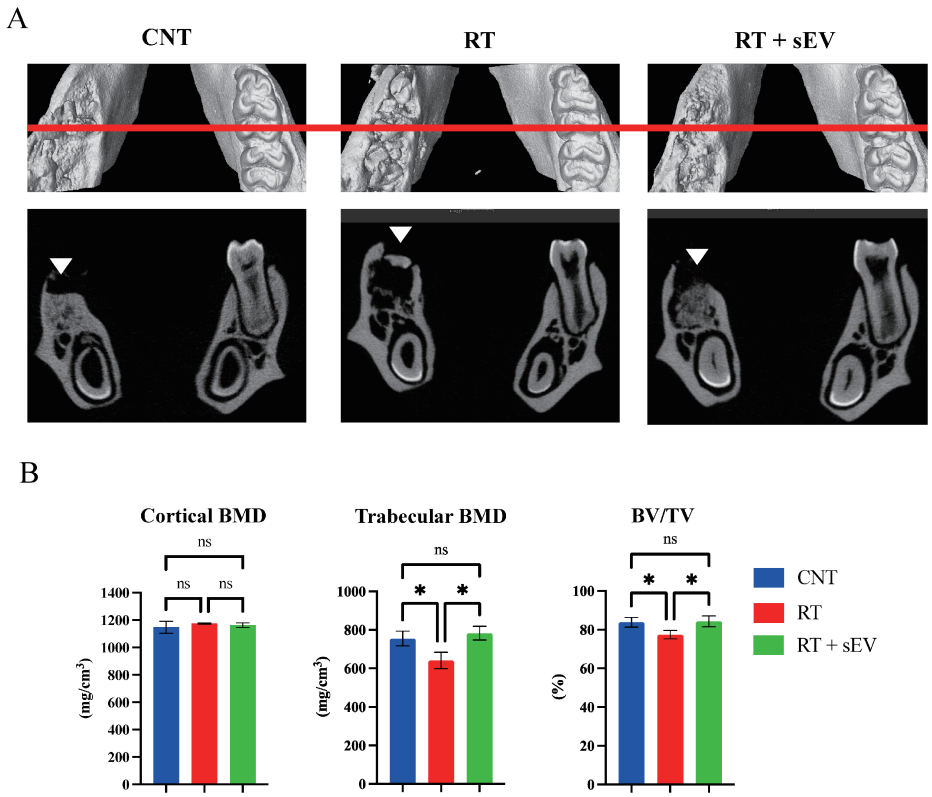

Fig. 4 Radiological evaluation of extraction socket in rat osteonecrosis of the jaw model

Fig. 4A: Three-dimensional reconstructed microtomography of the mandible using Latheta LCT-200 and representative coronal cross-sectional image. White arrowheads indicate the tooth-extracted parts.

Fig. 4B: The graph shows cortical/trabecular bone mineral density (BMD) and bone volume/tissue volume (BV/TV) in the extraction socket of the second molar according to the analysis software (VGSTUDIO 3.4, Volume Graphics GmbH).

All mandibles were evaluated 3 weeks after extraction. Control (CNT) group, rats with no irradiation and injected phosphate-buffered saline (PBS); Radiotherapy (RT) group, rats received 20 Gy irradiation and injected PBS; RT+ sEV group, rats received 20 Gy irradiation and injected human dental pulp stem cells -derived small extracellular vesicles (hDPSC-sEV). n = 3/group. Error bars indicate the SEM. $^{*}P < 0.05$.
ns: not significant

DISCUSSION

Radiation bone injuries may involve damage to MSC that contribute to wound healing.[29,30] ORNJ may be triggered by RT promoting the cellular senescence of MSC. SA-β-gal is a hydrolytic enzyme found specifically in senescent cells that converts β-galactosides to monosaccharides that accumulate in the lysosomes of senescent cells. In this study, the expression of SA-β-gal was enhanced in irradiated rBMC. Cellular senescence is defined as cell growth arrest induced when irreparable DNA damage occurs in proliferating cells. Our study has shown reduced cell proliferation rates in irradiated rBMC using colony formation and cell proliferation assays. Cell proliferation may be decreased by the high expression of molecules that arrest the cell cycle, specifically, p16 and p21, which act at checkpoints from the G1 to S phase and are the best-known senescence markers.[31,32] We observed an enhanced expression of these genes in

irradiated rBMC. These results indicate that radiation-induced cellular senescence in rBMC may follow this mechanism. To our knowledge, this study is the first to show that hDPSC-sEV may partially prevent cellular senescence in rBMC. Furthermore, hDPSC-sEV may be as effective as BMSC-sEV.[33,34]

Radiation-induced cellular senescence of BMSC may affect the cell quantity and quality due to reduced cell proliferative capacity. Some studies have suggested that irradiation disrupts the balance between adipogenic and osteogenic differentiation of BMSC, resulting in poor bone quality, which may cause ORNJ.[9,16,35] BMSC induced by cellular senescence preferentially differentiate into adipocytes rather than osteoblasts; thus, apoptotic bone cells and osteoblasts are not promptly replenished. Consequently, fatty marrow forms to replace the bone, facilitating ORNJ development. Herein, irradiated BMSC showed upregulated expression of adipogenesis-related genes, although bone differentiation-related genes were not upregulated. Concurrently, mRNA expression of osteodifferentiation-related genes in the BMSC treated with hDPSC-sEV immediately after irradiation was upregulated, and that of adipogenesis-related genes was downregulated. These results indicate that hDPSC-sEV can reconstitute the differentiation potential of irradiated BMSC.

In this study, we evaluated the efficacy of hDPSC-sEV in preventing tooth extraction after RT in a rat ORNJ model. In the RT group, bone exposure with mucosal defects in the extraction socket was observed, and histological evaluation revealed necrotic bone with increased vacuoles and fibrosis. Furthermore, there was a fatty marrow-like substance in some of the extraction sockets in the RT group; however, this was not observed in the RT+sEV group. Quantitative radiological analysis showed a decrease in trabecular bone density and bone mass ratio, whereas cortical bone density remained unchanged. These results are consistent with the clinical characteristics of ORNJ, indicating an appropriate ORNJ model for this study. Previous studies on osteoporosis in mouse femurs have shown that RT-induced cellular senescence causes a decrease in BV/TV.[36] In this study, we confirmed a decrease in bone density in rat mandibles due to RT and, by combining this with in vitro results, inferred that this effect is caused by cellular senescence. In contrast, in the RT+sEV group, both histological and radiological evaluation parameters showed partial recovery compared with those observed in the RT group. These findings are similar to those on the osteogenic effects of MSC grafting in extraction and bone defect formation models after RT,[9,12,37] suggesting that sEV may drive this effect. Specifically, wound closure and restoration of trabecular bone density indicate the restoration of the MSC wound-healing ability in the extraction socket, suggesting that hDPSC-sEV may provide an effective treatment for the jawbone after irradiation. In addition to active bone tissue regeneration, BMSC may contribute to the healing of osteonecrosis by promoting microvascular regeneration.[11,37] MSC can differentiate into endothelial cells and produce growth factors for angiogenesis, such as vascular endothelial growth factor and fibroblast growth factor, which promote hard and soft tissue healing ORNJ.[11] In this study, fewer new capillaries were suggested in the extraction socket of the RT group than those observed in the RT+sEV group. Therefore, any evaluations of the in vivo effects of hDPSC-sEV on MSC in extraction sockets may include angiogenesis assessments. However, there are several limitations to studies using this model. The model does not simulate the extraction of infected teeth, which in reality would account for the majority of the cases. Furthermore, patients may be undernourished after RT for oral cancer. These factors require consideration of the possibility that the extraction socket may be a more unfavorable environment for healing than this model.

Our results demonstrate the efficacy of the prophylactic administration of hDPSC-sEV, which may support the recovery of radiation-induced bone damage and promote wound healing after tooth extraction. hDPSC-sEV appear to have low toxicity, making them desirable as treatment compounds. In addition, BMSC-sEV[38-40] are non-tumorigenic and may enhance the suppressive ef-

fect of RT on tumor metastasis and transmit radiation-activated p53. Therefore, the administration of sEV immediately after RT may support antitumor effects of the RT. Furthermore, the bone regenerative effect of hDPSC-sEV on ORNJs may require administration immediately after irradiation or tooth extraction. A previous study using tonsil-derived MSC suggested that transplantation into the bone immediately after tooth extraction helped maintain tissue microenvironment suitable for bone regeneration.[12] In addition to the administration schedule used in this study, treatment with hDPSC-sEV immediately after tooth extraction may further promote bone regeneration in the extraction socket; however, further studies are required to confirm these effects. Providing multiple opportunities for the effective administration of hDPSC-sEV may help ensure the safety of tooth extraction in the post-RT jawbone. Establishing an effective method for administering hDPSC-sEV may support safe extractions after irradiation. However, while most cases of ORNJ are related to tooth extraction, some cases are caused by damage to the alveolar bone, chronic irritation, or infection. Therefore, delivering prophylactic treatment immediately after RT, as shown in this study, may improve patient prognosis by also preventing causes other than those related to tooth extraction.

This study suggests that the administration of hDPSC-sEV is effective in preventing ORNJ. One possible mechanism is that hDPSC-sEV inhibit radiation-induced cellular senescence in BMC.

COMPETING INTERESTS

The authors have no relevant financial or non-financial interests to disclose.

FUNDING

This study was supported by Japan Society for the Promotion of Science (JSPS) KAKENHI (grant numbers, JP19K10264, JP23K09394). The funder had no role in the study design; collection, analysis, or interpretation of data; in the writing of the report; or in the decision to submit the article for publication.

ACKNOWLEDGMENTS

We thank Division of Medical Research Engineering, Nagoya University Graduate School of Medicine, for their technical guidance. We also thank Center for Animal Research and Education (CARE) at Nagoya University, for technical supports for animal experiments.

REFERENCES

1 Mody MD, Rocco JW, Yom SS, Haddad RI, Saba NF. Head and neck cancer. *Lancet.* 2021;398(10318):2289–2299. doi:10.1016/S0140-6736(21)01550-6

2 Chronopoulos A, Zarra T, Ehrenfeld M, Otto S. Osteoradionecrosis of the jaws: definition, epidemiology, staging and clinical and radiological findings. A concise review. *Int Dent J.* 2018;68(1):22–30. doi:10.1111/idj.12318

3 Owosho AA, Tsai CJ, Lee RS, et al. The prevalence and risk factors associated with osteoradionecrosis of the jaw in oral and oropharyngeal cancer patients treated with intensity-modulated radiation therapy (IMRT): The Memorial Sloan Kettering Cancer Center experience. *Oral Oncol.* 2017;64:44–51. doi:10.1016/j.

oraloncology.2016.11.015
4 Curi MM, Dib LL. Osteoradionecrosis of the jaws: A retrospective study of the background factors and treatment in 104 cases. *J Oral Maxillofac Surg.* 1997;55(6):540–544. doi:10.1016/s0278-2391(97)90478-x
5 He Y, Ma C, Hou J, et al. Chinese expert group consensus on diagnosis and clinical management of osteoradionecrosis of the mandible. *Int J Oral Maxillofac Surg.* 2020;49(3):411–419. doi:10.1016/j.ijom.2019.06.015
6 He Y, Liu Z, Tian Z, Dai T, Qiu W, Zhang Z. Retrospective analysis of osteoradionecrosis of the mandible: Proposing a novel clinical classification and staging system. *Int J Oral Maxillofac Surg*. 2015;44(12):1547–1557. doi:10.1016/j.ijom.2015.04.006
7 Chrcanovic BR, Reher P, Sousa AA, Harris M. Osteoradionecrosis of the jaws-a current overview-part 1. *Oral Maxillofac Surg.* 2010;14(1):3–16. doi:10.1007/s10006-009-0198-9
8 Chamberlain G, Fox J, Ashton B, Middleton J. Concise review: Mesenchymal stem cells: Their phenotype, differentiation capacity, immunological features, and potential for homing. *Stem Cells*. 2007;25(11):2739–2749. doi:10.1634/stemcells.2007-0197
9 Zhang Y, Deng H, Yang Z, et al. Treatment of radiation bone injury with transplanted HUCB-MSCS via Wnt/ β-catenin. *Stem Cells Int.* 2021;2021:5660927. doi:10.1155/2021/5660927
10 Singh S, Kloss FR, Brunauer R, et al. Mesenchymal stem cells show radioresistance in vivo. *J Cell Mol Med.* 2012;16(4):877–887. doi:10.1111/j.1582-4934.2011.01383.x
11 Xu J, Zheng Z, Fang D, et al. Mesenchymal stromal cell-based treatment of jaw osteoradionecrosis in swine. *Cell Transplant.* 2012;21(8):1679–1686. doi:10.3727/096368911X637434
12 Park HS, Lee J, Kim JW, et al. Preventive effects of tonsil-derived mesenchymal stem cells on osteoradionecrosis in a rat model. *Head Neck.* 2018;40(3):526–535. doi:10.1002/hed.25004
13 Lener T, Gimona M, Aigner L, et al. Applying extracellular vesicle-based therapeutics in clinical trials – An ISEV position paper. *J Extracell Vesicles.* 2015;4:30087. doi:10.3402/jev.v4.30087
14 Valadi H, Ekström K, Bossios A, Sjöstrand M, Lee JJ, Lötvall JO. Exosome-mediated transfer of mRNAs and microRNAs is a novel mechanism of genetic exchange between cells. *Nat Cell Biol.* 2007;9(6):654–659. doi:10.1038/ncb1596
15 Raposo G, Stoorvogel W. Extracellular vesicles: Exosomes, microvesicles, and friends. *J Cell Biol.* 2013;200(4):373–383. doi:10.1083/jcb.201211138
16 Zuo R, Liu M, Wang Y, et al. BM-MSC-derived exosomes alleviate radiation-induced bone loss by restoring the function of recipient BM-MSCs and activating Wnt/β-catenin signaling. *Stem Cell Res Ther.* 2019;10(1):30. doi:10.1186/s13287-018-1121-9
17 Watanabe J, Sakai K, Urata Y, Toyama N, Nakamichi E, Hibi H. Extracellular vesicles of stem cells to prevent BRONJ. *J Dent Res.* 2020;99(5):552–560. doi:10.1177/0022034520906793
18 Gan L, Liu Y, Cui D, Pan Y, Zheng L, Wan M. Dental tissue-derived human mesenchymal stem cells and their potential in therapeutic application. *Stem Cells Int.* 2020;2020:8864572. doi:10.1155/2020/8864572
19 Shang F, Yu Y, Liu S, et al. Advancing application of mesenchymal stem cell-based bone tissue regeneration. *Bioact Mater.* 2021;6(3):666–683. doi:10.1016/j.bioactmat.2020.08.014
20 Jarmalavičiūtė A, Tunaitis V, Pivoraitė U, Venalis A, Pivoriūnas A. Exosomes from dental pulp stem cells rescue human dopaminergic neurons from 6-hydroxy-dopamine-induced apoptosis. *Cytotherapy.* 2015;17(7):932–939. doi:10.1016/j.jcyt.2014.07.013
21 Pivoraitė U, Jarmalavičiūtė A, Tunaitis V, et al. Exosomes from human dental pulp stem cells suppress carrageenan-induced acute inflammation in mice. *Inflammation.* 2015;38(5):1933–1941. doi:10.1007/s10753-015-0173-6
22 Shen Z, Kuang S, Zhang Y, et al. Chitosan hydrogel incorporated with dental pulp stem cell-derived exosomes alleviates periodontitis in mice via a macrophage-dependent mechanism. *Bioact Mater.* 2020;5(4):1113–1126. doi:10.1016/j.bioactmat.2020.07.002
23 Dong J, Sakai K, Koma Y, et al. Dental pulp stem cell-derived small extracellular vesicle in irradiation-induced senescence. *Biochem Biophys Res Commun.* 2021;575:28–35. doi:10.1016/j.bbrc.2021.08.046
24 Zhang L, Chan C. Isolation and enrichment of rat mesenchymal stem cells (MSCS) and separation of single-colony derived MSCs. *J Vis Exp.* 2010;37:1852. doi:10.3791/1852
25 Ohara G, Okabe K, Toyama N, et al. Stem cell therapy based on human periodontal ligament stem cells preactivated with TNF-α as for human head and neck squamous cell carcinoma. *J Oral Maxillofac Surg Med Pathol.* 2024;36(2):217–226. doi:10.1016/j.ajoms.2023.08.006
26 Ohara G, Okabe K, Toyama N, et al. Hyperthermia maintains death receptor expression and promotes TRAIL-induced apoptosis. *J Oral Pathol Med*. 2023;52(8):718–726. doi:10.1111/jop.13457
27 Yamasaki MC, Roque-Torres GD, Peroni LV, et al. A modified protocol of mandibular osteoradionecrosis in-

duction in rats with external beam radiation therapy. *Clin Oral Investig.* 2020;24(4):1561–1567. doi:10.1007/s00784-019-03054-0

28 Sønstevold T, Johannessen CA, Stuhr L. A rat model of radiation injury in the mandibular area. *Radiat Oncol.* 2015;10:129. doi:10.1186/s13014-015-0432-6

29 Suva LJ, Griffin RJ. The irradiation of bone: Old idea, new insight. *J Bone Miner Res.* 2012;27(4):747–748. doi:10.1002/jbmr.1586

30 Zou Q, Hong W, Zhou Y, et al. Bone marrow stem cell dysfunction in radiation-induced abscopal bone loss. *J Orthop Surg Res.* 2016;11:3. doi:10.1186/s13018-015-0339-9

31 Yu KR, Kang KS. Aging-related genes in mesenchymal stem cells: a mini-review. *Gerontology.* 2013;59(6):557–563. doi:10.1159/000353857

32 Lunyak VV, Amaro-Ortiz A, Gaur M. Mesenchymal stem cells secretory responses: Senescence messaging secretome and immunomodulation perspective. *Front Genet.* 2017;8:220. doi:10.3389/fgene.2017.00220

33 Dorronsoro A, Santiago FE, Grassi D, et al. Mesenchymal stem cell-derived extracellular vesicles reduce senescence and extend health span in mouse models of aging. *Aging Cell.* 2021;20(4):e13337. doi:10.1111/acel.13337

34 Liao CM, Luo T, von der Ohe J, de Juan Mora B, Schmitt R, Hass R. Human MSC-derived exosomes reduce cellular senescence in renal epithelial cells. *Int J Mol Sci.* 2021;22(24):13562. doi:10.3390/ijms222413562

35 Wang Y, Zhu G, Wang J, Chen J. Irradiation alters the differentiation potential of bone marrow mesenchymal stem cells. *Mol Med Rep.* 2016;13(1):213–223. doi:10.3892/mmr.2015.4539

36 Yao Z, Murali B, Ren Q, et al. Therapy-Induced Senescence Drives Bone Loss. *Cancer Res.* 2020;80(5):1171–1182. doi:10.1158/0008-5472.CAN-19-2348

37 Jin IG, Kim JH, Wu HG, Kim SK, Park Y, Hwang SJ. Effect of bone marrow-derived stem cells and bone morphogenetic protein-2 on treatment of osteoradionecrosis in a rat model. *J Craniomaxillofac Surg.* 2015;43(8):1478–1486. doi:10.1016/j.jcms.2015.06.035

38 de Araujo Farias V, O'Valle F, Serrano-Saenz S, et al. Exosomes derived from mesenchymal stem cells enhance radiotherapy-induced cell death in tumor and metastatic tumor foci. *Mol Cancer.* 2018;17(1):122. doi:10.1186/s12943-018-0867-0

39 Azzam EI, de Toledo SM, Gooding T, Little JB. Intercellular communication is involved in the bystander regulation of gene expression in human cells exposed to very low fluences of alpha particles. *Radiat Res.* 1998;150(5):497–504. doi:10.2307/3579865

40 Mothersill C, Seymour CB. Cell-cell contact during gamma irradiation is not required to induce a bystander effect in normal human keratinocytes: evidence for release during irradiation of a signal controlling survival into the medium. *Radiat Res.* 1998;149(3):256–262. doi:10.2307/3579958